Journal of Photochemistry and Photobiology 13 (2023) 100152

Contents lists available at ScienceDirect

Journal of Photochemistry and Photobiology

journal homepage: www.sciencedirect.com/journal/journal-of-photochemistry-and-photobiology

Elucidating the photosynthetic responses in chlorophyll-deficient soybean (Glycine max, L.) leaf

Kelvin Acebron [a,*], Nicole Salvatori [b,c], Giorgio Alberti [b,d], Onno Muller [a], Alessandro Peressotti [b], Uwe Rascher [a], Shizue Matsubara [a]

[a] Institute of Bio- and Geosciences, IBG-2: Plant Sciences, Forschungszentrum Jülich GmbH, Leo-Brandt-Str, 52425, Jülich, Germany
[b] Department of Agricultural, Food, Environmental and Animal Sciences, University of Udine, Via delle Scienze 206, 33100, Udine, Italy
[c] Department of Life Sciences, University of Trieste, 34127, Trieste, Italy
[d] Faculty of Science and Technology, Free University of Bolzano, Bolzano, Italy

ARTICLE INFO

Keywords:
Non-photochemical quenching (NPQ)
Photochemical quenching
Effective quantum yield of photosystem II (Φ_{PSII})
Electron transport rate (ETR)
Solar-induced fluorescence (SIF)

ABSTRACT

Chlorophyll (Chl)-deficient plants can potentially increase global surface albedo of mono-cropping systems, and simultaneously maintain a similar photosynthetic efficiency by increasing light canopy penetration and thus lowering investment in pigments. However, some previous studies have shown that pale mutants might reduce productivity in field conditions. Such lower yields were suspected to be due to loss of photosynthetic efficiency at leaf level during light fluctuations as a consequence of reduced capacity and slower relaxation of non-photochemical quenching (NPQ) of Chl fluorescence. In this paper, we tested this hypothesis by comparing, CO_2 assimilation (A), photosystem II (PSII) efficiency (Φ_{PSII}), photochemical quenching and NPQ, electron transport rate (ETR) and fluorescence yield (F_{yield}) in a green soybean (*Glycine max* L.) cultivar (Eiko) and in a Chl-deficient (MinnGold) mutant under dynamically fluctuating light conditions. MinnGold had significantly slower induction of ETR and lower A and ETR than Eiko, but there was little difference in Φ_{PSII} between the two genotypes, suggesting that the lower photosynthesis of MinnGold was mainly due to lower light energy absorption by a Chl-deficient leaf. The NPQ capacity was also smaller in MinnGold than in Eiko. As for the kinetics of the rapidly inducible component of NPQ, MinnGold showed slower induction, not relaxation, than Eiko. The combination of the effect of Chl-deficiency on lower photosynthesis, NPQ capacity and slower NPQ induction may explain the lower biomass accumulation of MinnGold in the field. Our physiological observations, combined with fluorescence kinetics, can serve as a basis to parameterize Chl content in modelling radiative transfer and photosynthesis for upscaling measures of plant and ecosystem productivity by a big leaf model.

Introduction

Pale-green plants, i.e. varieties that can reflect more light than their conventional ancestors, have been proposed as a possible solar radiation management strategy to reduce negative impacts of climate change [1, 2]. Yet, the idea of enhancing leaf reflectance and transmittance by reducing the concentration of light-absorbing pigments in leaves is only appealing if photosynthesis and yield are not negatively affected by such a reduction. In fact, photosynthetic rates of plant leaves have often been related to their chlorophyll (Chl) content [3]. Contrary to this notion, recent papers have shown that Chl-deficient mutants may exhibit similar or even higher carbon (C) uptake rates and biomass accumulation than their reference wild types, albeit not consistently (see comparative studies in [4–6]). The higher C uptake was attributed to a better distribution of light within the canopy [7–9] and thus to an increase in photosynthetic light-use efficiency of the plant as a result of reduced light-harvesting antenna size in upper-canopy leaves [10]. However, other studies have reported lower leaf photosynthetic rates in Chl-deficient mutants [11] or reduced crop yields even with similar photosynthesis and respiration at leaf scale or at canopy scale under steady-state conditions [12]. These contrasting results call for identification of physiological mechanisms behind possible yield gaps in pale-green plants. Understanding these mechanisms is a precondition to successfully apply genome editing to create Chl-deficient plants with improved productivity for effective solar radiation management.

Journal: Journal of Photochemistry and Photobiology (Special Issue on Chlorophyll fluorescence and Photosynthesis)
* Corresponding author.
E-mail addresses: kacebron@gmail.com, kacebron@gmail.com (K. Acebron).

https://doi.org/10.1016/j.jpap.2022.100152

Available online 9 November 2022
2666-4690/© 2022 Published by Elsevier B.V. This is an open access article under the CC BY-NC-ND license (http://creativecommons.org/licenses/by-nc-nd/4.0/).

List of the most important abbreviations

A	net CO_2 assimilation rate
ChlF	chlorophyll fluorescence
C_i	calculated CO_2 concentration inside the leaf
ETR	electron transport rates estimated by fluorescence
g_s	stomatal conductance
J_a	electron transport rates estimated by gas exchange
F_{yield}	fluorescence yield
F_v/F_m	maximal efficiency of PSII
NPQ	non-photochemical quenching
qL	fraction of open PSII reaction centers according to the lake model
qP	photochemical quenching, fraction of open PSII reaction centers according to the puddle model
qPd	qP in the dark following light exposure
Φ_D	efficiency of basal heat dissipation
Φ_f	efficiency of fluorescence emission
Φ_{NPQ}	efficiency of regulated heat dissipation
Φ_{PSII}	operating efficiency of PSII

Two recent studies [12,13] focusing on a Chl-deficient soybean (*Glycine max* (L.) Merr.) variety MinnGold have attributed the lower crop yield measured in the field to seemingly slower relaxation of photo-protective non-photochemical quenching (NPQ) during light fluctuations. More in general, for soybean crop canopies, this slow NPQ relaxation upon sun–shade transitions was calculated to cost >11% of daily carbon assimilation [14]. If this is the case, accelerating NPQ adjustments might increase the photosynthetic C uptake and hence biomass in either green or Chl-deficient plants [15]. Maximizing photosynthetic light-use efficiency in fluctuating light environments, while avoiding photo-inhibition, necessitates fast adjustments and coordination of the light reactions and CO_2 assimilation [16]. The strategy to accelerate NPQ induction and relaxation has been applied to both tobacco [17] and soybean plants [15] to improve C gain and biomass, although the same approach resulted in decreased biomass accumulation in *Arabidopsis* [18]. This implies that there are still missing gaps on understanding the link between Chl concentration, its effect on the balance between NPQ and photosynthesis and its consequence on plant productivity. Radiative transfer and photosynthesis models may fill this gap, but linking light absorption by Chl to the three energy dissipation pathways (fluorescence, photosynthesis and NPQ) still needs further investigation.

After light energy absorption by photosynthetic pigments, excitation energy transfer is influenced by the connectivity between photosystem complexes [19,20]. The lake model assumes infinite excitonic connectivity among all PSII reaction centers via shared light-harvesting antennae, whereas the puddle model is based on excitonically separate PSII units [20,21]. To date, we do not know which model, or an intermediate between the two, can better describe the situation in different plant species under various environmental conditions. Nevertheless, Chl fluorescence (ChlF) parameters like qP and qL (based on the puddle and lake model, respectively; [20,21]) are being used to estimate the fraction of open PSII centers (with the primary quinone acceptor Q_A oxidized) performing photochemical quenching. Given the function of Chl for light harvesting, Chl deficiency may alter the partitioning of absorbed light energy between PSII and PSI, or the excitation energy transfer between PSII reaction centers. These factors are also relevant for understanding passive solar-induced fluorescence (SIF) signal. While the quantum yield of ChlF emission at PSII (Φ_f) is defined by the rate constants of photochemical (k_{PSII}) and non-photochemical processes (k_{NPQ} and k_D for regulated and non-regulated processes, respectively), measured ChlF intensity (F) is also influenced by additional factors, including light intensity, leaf absorbance, the fraction of light energy absorbed by PSII ($fraction_{PSII}$), and reabsorption of emitted ChlF [22,23].

In this paper, we tested the hypothesis that Chl-deficient plants have slower adjustment of photosynthetic light energy harvesting under fluctuating light conditions. Working on this hypothesis enabled us to explore in detail the morphological and physiological differences between Chl-deficient and green leaf. We used the soybean variety MinnGold [12] that has ~80% less Chl contents than green varieties and grew it in growth chambers with light regimes similar to what we used in leaf cuvette for photosynthesis measurement. In particular, we measured plants grown either in fluctuating or non-fluctuating light conditions to test if the growing conditions are affecting the measurements thus reducing the artifacts. The effects of Chl deficiency on excitation energy partitioning and linear electron transport were studied by combining ChlF and leaf gas exchange measurements under dynamically fluctuating light conditions. The parameters were assessed during photosynthetic induction (dark-to-light transitions) and during light fluctuations in the minute range.

Materials and Methods

Plant materials and growth conditions

The pale-green mutant MinnGold and the green variety Eiko were sown in pots (13 × 13 × 18 cm) and grown inside two 0.54 m^3 growth chambers (16 pots $chamber^{-1}$) under fluctuating (FL) and non-fluctuating (NFL) light, respectively (for a detailed description of the system, see [24]; and environmental conditions are shown in Fig. S1). The LED system within each chamber was set to simulate a fixed daily profile (June 21st) at a latitude of 46.07° N and a longitude of 13.23° E with a maximum photosynthetic photon flux density (PPFD) of 650 μmol m^{-2} s^{-1} at noon (NFL treatment). This target value was chosen because, according to the data provided by [12], this light intensity is not saturating and allows to prevent photoinhibition, thus to ensure that the measured responses were only due to the applied light fluctuations. In FL, light fluctuated ±20% with a period of 60 s around the hourly value set in NFL. By doing this, plants grown either in FL or NFL received the same cumulative light intensity throughout the day. The 20% in light fluctuations were also chosen mainly to avoid photoinhibition [12] and thus only affecting the reversible component of NPQ (qE). Moreover, the 1-minute fluctuation was chosen to stress the photosynthesis itself (in particular the light phase) rather than other processes such as stomatal conductance, whose response is an order of magnitude slower [25]. Three plants from each treatment were randomly selected 24 days after sowing and dark-adapted prior to the leaf-level measurements of ChlF and gas exchange described below.

Morphological measurements

Mean plant height and mean leaf area per treatment, as well as leaf Chl content, were measured 4 or 5 times during the experiments on three randomly selected plants or leaves in each chamber, respectively. Plant heights was measured with a meter stick, the leaf area was calculated by approximating the leaf to a rhombus and therefore by measuring its major (M) and minor (m) diagonals, while the Chl content was measured using a SPAD.

Leaf-level gas-exchange and fluorescence measurement

On the three randomly chosen plants for each treatment 24 days after sowing, young and fully expanded leaves were selected to measure the quantum yield of ChlF and gas-exchange parameters during light induction. Measurements were done using a LI-6800 (Licor Biosciences, Nebraska, USA) equipped with an infra-red gas analyzer coupled with pulse-amplitude modulation (PAM) fluorometer. All plants were dark-adapted overnight prior to measurements. Before turning on the

actinic light inside the leaf cuvette, measuring beam (< 1 μmol m^{-2} s^{-1}) was turned on to obtain the minimal fluorescence yield F_0 and a short saturating flash (> 6,000 μmol m^{-2} s^{-1}) of 800 ms was given to obtain the maximal fluorescence yield in the dark-adapted state (F_m). The maximal efficiency of PSII (F_v/F_m) was calculated according to Eq. (1) [26].

$$F_v \Big/ F_m = \frac{(F_m - F_0)}{F_m} \tag{1}$$

Dark respiration rate was measured before the onset of illumination. During light induction using constant intensity of red (94%) and blue (6%) light (650 μmol m^{-2} s^{-1}), CO_2 level inside the leaf cuvette was maintained at 400 μmol mol^{-1}, vapor pressure deficit of the leaf was set to 1.8 kPa and leaf temperature at 25°C. For measurements in fluctuating light, all environmental parameters were the same except that the light intensity was changing between 780 μmol m^{-2} s^{-1} and 520 μmol m^{-2} s^{-1} with a period of 60 s, similarly to the conditions within the growth chambers. Gas-exchange and ChlF measurements were recorded for 60 min after turning on the light inside the cuvette and for another 6 min after light was turned off. Throughout the whole measurement period (60 min light + 6 min dark), 800-ms saturating light of > 6,000 μmol m^{-2} s^{-1} was applied onto the leaf every 20 s to measure the maximal fluorescence yield in the light (F'_m) and dark (F_m). The operating efficiency of PSII (Φ_{PSII}) was then calculated using Eq. (2), where F_s is the steady-state fluorescence yield recorded after the measuring beam under the actinic light [27].

$$\Phi_{PSII} = \frac{(F'_m - F_s)}{F'_m} \tag{2}$$

NPQ was calculated according to [28] based on the Stern-Volmer method (Eq. (3)).

$$NPQ = \frac{(F_m - F'_m)}{F'_m} \tag{3}$$

To analyze the NPQ kinetics, we fitted the data with single or double exponential curves as in [29]. The following equation was used to analyze NPQ induction in dark-adapted leaves upon illumination:

$$NPQ_i = y_0 + A_1 * \left(1 - exp\left(-\frac{t}{\tau_1}\right)\right) \tag{4}$$

We assumed $y_0 = 0$ since the induction was measured in dark-adapted leaves. We used a single exponential function for the NPQ induction in Eiko and MinnGold. For NPQ relaxation during the 5-min leaf darkening following 1-h light protocol, the following equation was used:

$$NPQ_r = y_0 + A_1 * exp\left(-\frac{t}{\tau_1}\right) + A_2 * exp\left(-\frac{t}{\tau_2}\right) \tag{5}$$

Three different components were assumed in NPQ relaxation; a fast component which is related to the rapidly reversible qE component described by the amplitude A_1 and the time constant (lifetime) τ_1, a second component which is presumably linked to the conversion of violaxanthin to zeaxanthin described by A_2 and τ_2, and a slow component which is regarded as the photoinhibitory component of NPQ (qI) described by y_0 [29]. The fitting was done in MATLAB2019 (fminsearch).

The electron transport rates estimated by ChlF (ETR, Eq. (6)) and by CO_2 gas exchange (J_a, Eq. (7)) were also calculated based on the methods described in [30] and [31], respectively.

$$ETR = I * fraction_{PSII} * \alpha * \Phi_{PSII} \tag{6}$$

$$J_a = \left(4.5 * \frac{\left(C_i + \frac{7\Gamma^*}{3}\right)}{(C_i - \Gamma^*)}\right) * (A + R_d) \tag{7}$$

ETR is a function of the incident light intensity (I), the fraction of absorbed light received by PSII ($fraction_{PSII}$) which is normally set to 0.5 [32], and the absorbance coefficient (α) which was set to 0.55 for MinnGold and 0.78 for Eiko, as calculated in the growth chambers [24]. On the other hand, J_a is a function of the respiration in the dark (R_d), the net CO_2 assimilation (A), CO_2 concentration inside the leaf (C_i), and the CO_2 compensation point (Γ^*) in the absence of dark respiration [33]. Γ^* was set to 43.67 μmol mol^{-1} according to the Γ^* of *Glycine max* used by [34] (converted from the Pa units using the conversion table from [35]).

The efficiency of each energy dissipation pathway was determined throughout the photosynthetic induction. We assumed that the sum of the quantum yield of ChlF emission (Φ_f, in Eq. (8); [19]), PSII photochemistry (Φ_{PSII} in Eq. (2); [27]), regulated heat dissipation (Φ_{NPQ} in Eq. (9); [4,28,36]) and basal heat dissipation (Φ_D in Eq. (11)) is equal to unity (Eq. (12)).

$$\Phi_f = \frac{(F_s - F_0)}{(F_m - F_0)} \tag{8}$$

$$\Phi_{NPQ} = \left(\frac{F_s}{F'_m}\right) - \left(\frac{F_s}{F_m}\right) \tag{9}$$

$$\Phi_{f,D} = \frac{F_s}{F_m} \tag{10}$$

$$\Phi_D = \Phi_{f,D} - \Phi_f \tag{11}$$

$$1 = \Phi_f + \Phi_{PSII} + \Phi_{NPQ} + \Phi_D \tag{12}$$

Finally, the fraction of open PSII reaction centers was computed on the basis of either the puddle model (qP, Eq. (13)) or the lake model (qL, Eq. (14)). The calculations were adopted from [19].

$$qP = \frac{(F'_m - F_s)}{(F'_m - F'_{0calc})} \tag{13}$$

$$qL = \frac{\frac{1}{F_s} - \frac{1}{F'_m}}{\frac{1}{F'_{0calc}} - \frac{1}{F'_m}} = \frac{(F'_m - F_s)}{(F'_m - F'_{0calc})} * \frac{F'_{0calc}}{F_s} \tag{14}$$

Both Eqs. (13) and (14) require estimation of the minimal fluorescence yield in a light adapted state (F'_0) which was calculated in this study ($F'_{0\ calc}$) according to [37].

$$F'_{0calc} = \frac{1}{\left(\frac{1}{F_0} - \frac{1}{F_m} + \frac{1}{F'_m}\right)} \tag{15}$$

Calculating photoprotection of NPQ after photosynthetic light induction

We evaluated the difference in photoprotection between Eiko and MinnGold during the dark period following the light treatment by using the parameter qPd (qP in the dark after light exposure [38]), also called PI (photoprotection index [15]).

$$qPd = \frac{(F'_m - F'_{0act})}{(F'_m - F'_{0calc})} \tag{16}$$

where $F'_{0\ act}$ is the measured actual F'_0 in the dark following light exposure. qPd range from 0 to 1 where 1 indicates that no photoinhibition occurred [38] and NPQ was fully effective [15].

Statistical tests

Pairwise mean comparisons between MinnGold and Eiko were performed using *Welch* two-sample t-test in R software (R Core Team, 2016) for all the parameters described above.

Results

Plant morphology and the effect of fluctuating light on Soybean growth

Even if the two varieties show a clear difference in the color of the leaves and on their Chl content (Fig. 1), FL treatment did not significantly affect the growth. In fact, although there was an obvious height advantage of Eiko (i.e. Eiko were taller than MinnGold especially at later stage), both plants did not grow better under NFL. Seemingly, leaf area followed a similar trend with the exemption that, in later stage before final harvest, Eiko plants grown in FL had larger leaf area than the ones grown under NF and MinnGold plants in FL were apparently taller than the ones grown under NFL (Fig. S2).

Excitation energy transfer during photosynthetic induction

We first analyzed the effects of Chl deficiency on photosynthetic induction. Upon illumination of dark-adapted plants, Φ_{PSII} increased in both varieties equally (Fig. 2a), even if the fluorescence parameters were corrected based on the contribution of PSI (data not shown). Thereafter, MinnGold showed slightly higher Φ_{PSII} until similar steady-state levels were reached in both varieties (Fig. S3a). As expected, the fraction of open PSII centers was larger when it was estimated by the puddle model (qP; Fig. 2b) than by the lake model (qL; Fig. 2c) [19]. Interestingly, qP was nearly identical in the two varieties (Fig. 2b), while qL was smaller in MinnGold (Fig. 2c). In addition, the light-induced formation of NPQ peaked in Eiko after ~10 min before starting to decline gradually and continuously (Fig. S3d). The low NPQ of MinnGold showed a saturation curve. Similar to Φ_{PSII}, this trend remained the same even if we corrected for the contribution of PSI. Furthermore, we noticed that leaf temperature was unstable during the measurements of Eiko, which may have resulted in the discontinuous induction traces of this variety (Fig. S3). Nevertheless, this did not change the general trends described above.

Energy partitioning after induction

To understand the effect of Chl deficiency on energy partitioning at PSII level, we then analyzed the quantum yield of the four energy dissipation processes, Φ_{PSII}, Φ_{NPQ}, Φ_f, and Φ_D, after 11 minutes of photosynthetic induction. MinnGold had lower Φ_D and Φ_{NPQ} and higher Φ_f than Eiko (all $p<0.001$; Table 1), while no significant difference in Φ_{PSII} was found between the two varieties. Contrary to the higher Φ_f at PSII but in accordance with less light absorption, the apparent F_{yield} at leaf level was significantly lower ($p< 0.001$) in MinnGold (Table 1). As seen for Φ_{NPQ} and Φ_{PSII}, lower NPQ ($p<0.001$) was measured in MinnGold but F_v/F_m was comparable ($p=0.053$) (Table 1). In fact, these plants had similar F_v/F_m values regardless of whether they were grown under, and thus acclimated to, the NFL or FL conditions (Table S1). Consistent with the reduced NPQ capacity, MinnGold was less efficient in photoprotection, as assessed by the parameter qPd ($p=0.0088$) following 1-h light exposure to the constant (650 μmol m^{-2} s^{-1}) or fluctuating light (changing between 780 and 520 μmol m^{-2} s^{-1} every 60 s) with a train of > 6000 μmol m^{-2} s^{-1} saturation pulses applied every 20 s to measure F'_m. Still, F_v/F_m decline was similar in both genotypes after these treatments (Table S1).

Comparison of electron transport rates obtained by ChlF versus CO_2 gas exchange

The rate of linear electron transport was calculated from Φ_{PSII} (ETR; Fig. 2e) or CO_2 gas exchange (J_a; Fig. 2f) measured during the photosynthetic induction. Both traces largely paralleled the changes in Φ_{PSII} (Fig. 2a), although the values were always higher in Eiko than in MinnGold. Between the two types of electron transport parameters, the values were initially similar but ETR became substantially lower than J_a after 10 min. A peculiar feature found in MinnGold, but not in Eiko, was the delayed increase in J_a around 10 min after the onset of light exposure (Fig. 2f). This pattern also appeared in the net CO_2 assimilation (A; Fig. 2g), together with a delayed increase in stomatal conductance (g_s) in MinnGold (Fig. S3h). While the initial g_s in the dark and during the first ~10 min of illumination was somewhat higher in MinnGold than in Eiko (Fig. 2h), it remained lower in MinnGold the rest of the time (Fig. S3h). The calculated CO_2 concentration inside the leaf (C_i) stayed at ~300 μmol mol^{-1} in both cultivars at steady state, after an initial decline in the first 10 min and recovery until 20 or 30 min in Eiko and MinnGold, respectively (Fig. 2i).

The distinct induction patterns of ETR and J_a found in MinnGold and Eiko (Fig. 2e, f) prompted us to plot these two parameters against each other. The relationship fell initially onto a 1:1 ratio but with substantial deviations at high values (Fig. 3). The deviations emerged in both varieties 10-15 min after dark-to-light transition. Thereafter, J_a was always higher than ETR in Eiko. In contrast, some data points of MinnGold were above the 1:1 line, corresponding to the sluggish J_a increase observed in this variety after ~10 min (Fig. 2f). Beyond this point, however, MinnGold showed the same picture as seen in Eiko (ETR<J_a).

Finding this discrepancy, we then analyzed the product of $fraction_{PSII}$ * α – the two parameters in the ETR calculation (Eq. (6)). This product is normally considered as constant (typically 0.42, assuming 0.5 for $fraction_{PSII}$ and 0.84 for α), although it is known to be an unvalidated approximation [30]. By combining Eqs. (6) and (7), we calculated this product as a dynamic parameter that accounts for the deviations from the 1:1 relationship found in Fig. 3 (Supplementary Note 1). Fig. S4 shows how this product changed, especially during the first 30 min of photosynthetic induction from a dark-adapted state. A steep decline in

Type	Eiko	MinnGold
Chl content (SPAD units)	36.75 ± 0.54	15.25 ± 0.55

Fig. 1. Photos of the two cultivars inside the growth chambers and their Chl contents.

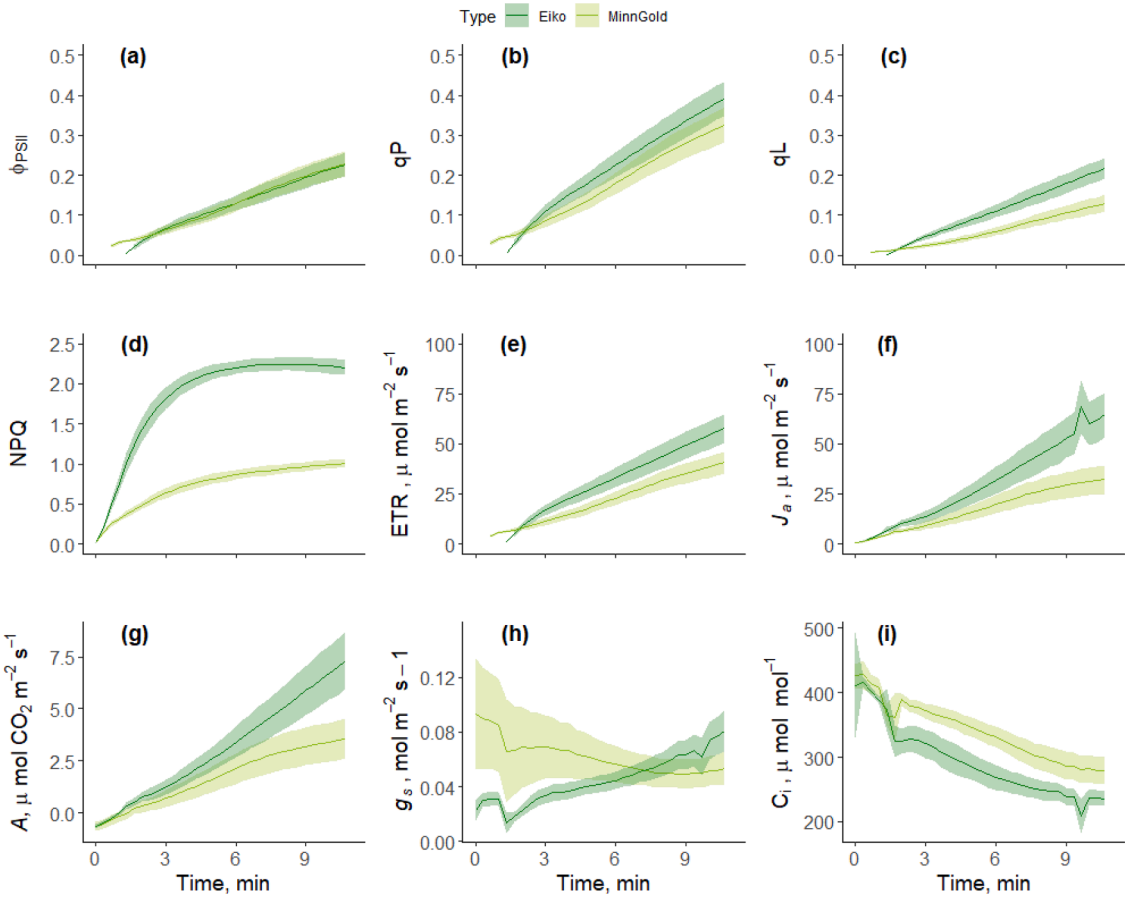

Fig. 2. Analysis of ChlF and CO_2 gas exchange during the initial phase of photosynthetic induction in the green variety Eiko and MinnGold. (a) Operating efficiency of PSII, Φ_{PSII}, (b) open fraction of PSII based on the puddle model, qP, or (c) the lake model, qL, (d) NPQ, (e) PSII electron transport rate, ETR, estimated from Φ_{PSII}, (f) actual electron transport rate, J_a, derived from gas exchange data, and (g) net CO_2 assimilation rate, A, (h) stomatal conductance, g_s, and (i) calculated CO_2 concentration inside the leaf, C_i. Plants were grown in either the NFL or the FL condition and dark-adapted overnight prior to the measurements. Since no significant effect of the growth light conditions was found (Table 1), data of all plants (n=6) were combined for each genotype. During the induction, light intensity was maintained at 650 μmol m^{-2} s^{-1}. The solid lines show the average values and the pale areas represent the standard errors.

Table 1
Differences in the fluorescence parameters between Eiko and Chl-deficient mutant MinnGold under steady-state conditions. The values are means ± standard errors (n=6). Different letters indicate a significant difference between the two varieties ($p<0.05$).

Fluorescence parameters	Eiko	MinnGold
F_{yield}	948.7 ± 23.9^a	680.5 ± 31.1^b
NPQ	2.17 ± 0.10^a	1.03 ± 0.05^b
F_v/F_m	0.812 ± 0.004^a	0.825 ± 0.005^a
qPd	0.837 ± 0.010^a	0.793 ± 0.009^b
Φ_f	0.062 ± 0.007^a	0.241 ± 0.021^b
Φ_{NPQ}	0.517 ± 0.027^a	0.380 ± 0.017^b
Φ_D	0.177 ± 0.007^a	0.133 ± 0.005^b
Φ_{PSII}	0.244 ± 0.029^a	0.246 ± 0.033^a

the first ~ 4 min was followed by a slow increase before reaching a steady state after ~20 or ~30 min in Eiko and MinnGold, respectively. The onset of the increase was delayed in MinnGold by ~10 min compared to Eiko. As expected, MinnGold had generally lower *fraction$_{PSII}$* * α than Eiko throughout the induction (Fig. S4).

Adjustments of photosynthetic light use during light fluctuations

To evaluate the effect of Chl deficiency on adjustment of absorbed light energy partitioning at PSII, we compared Φ_f, Φ_{PSII}, Φ_D and Φ_{NPQ} in MinnGold and Eiko during the induction in fluctuating light or constant light (Fig. 4). By calculating the areas under the curves of individual components, we found, for each variety, no significant difference in energy partitioning between the two light treatments of photosynthetic induction or between the two growth light conditions (Table S2). Both varieties exhibited their typical energy partitioning patterns in the fluctuating light as well as in the constant light condition (Fig. 4).

To test whether Chl-deficiency alters the kinetics of NPQ adjustment, we analyzed time constants (τ) of NPQ induction and relaxation in constant light and subsequent leaf darkening. Both induction and relaxation of NPQ were fitted to exponential functions: the induction data indicated the presence of a single dominant component (Eq. (4)), while two exponential components were needed to describe the relaxation data (Eq. (5)). During induction, MinnGold had a smaller amplitude (A_1) and a longer τ_1 compared to Eiko (Table 2), suggesting a reduced capacity and slower formation of rapidly inducible qE in Chl-deficient leaves upon light exposure. No significant difference was found between the two varieties during dark relaxation (Table 2).

Notably, Φ_{PSII} was similar for both types during the induction phase (Fig. 5a), although the values tended to be slightly but reproducibly higher in MinnGold under both 780 and 520 μmol m^{-2} s^{-1} of the fluctuating light treatment after >20-min light exposure (Fig. S5a). While the difference in Φ_{PSII} slowly disappeared in 520 μmol m^{-2} s^{-1}, Φ_{PSII} of MinnGold remained higher in 780 μmol m^{-2} s^{-1}. Slightly higher Φ_{PSII} of MinnGold is also seen in Figs. S3a. The largest difference in Φ_{PSII} was observed ~30 min after dark-to-light transition (Figs. S3a and S5a), much later than the largest difference in Φ_{NPQ} was recorded (Figs. 5b

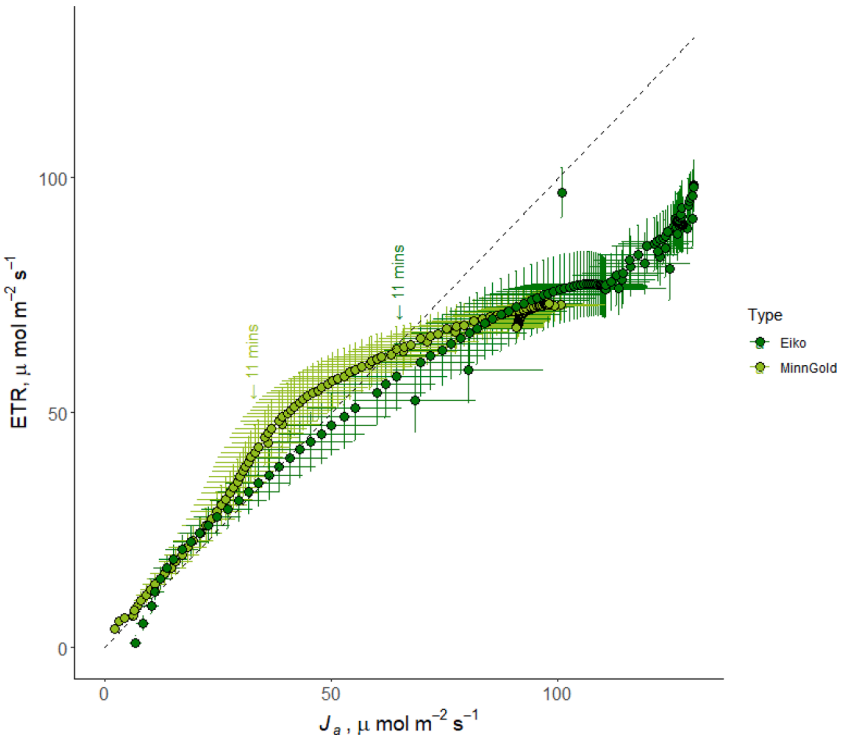

Fig. 3. Correlation between ETR and J_a. Data were collected in Chl-deficient leaves of MinnGold (light green) and green leaves of Eiko (dark green) during photosynthetic induction under constant illumination at 650 μmol m^{-2} s^{-1} (cf. Fig. 1e, f). The dashed line shows the 1:1 relationship. Symbols and vertical/horizontal bars represent means and standard errors, respectively (n=6).

and S5b). In this case, to compare the dissipative processes to the quantum yield of PSII (Φ_{PSII}) we show the quantum yield of the light-induced NPQ, Φ_{NPQ}, as it is representative of the qE component of NPQ [36].

Discussion

How does Chl deficiency affect light harvesting and photoprotection?

The bulk of Chl molecules is embedded in pigment-protein complexes to absorb and transfer light energy to the reaction centers of PSII and PSI. The puddle model, which is based on excitonically independent PSII units, calculated similar fractions of open PSII centers in MinnGold and Eiko during the induction (Fig. 2b). The lake model, which assumes infinite excitonic connectivity among all PSII centers, indicated that the fraction of open PSII centers was smaller in MinnGold than in Eiko (Fig. 2c). The qP and qL differed substantially (by ~50%) in each variety, as is expected when the open PSII fraction is small [19]. It therefore seems that, upon dark-to-light transition, excitonic connectivity among (mostly closed) PSII centers approaches, at least initially, the situation of qP and the puddle model. The underestimation of qL in MinnGold (Fig. 2c) suggests lower actual connectivity of PSII centers in Chl-deficient leaves. This is in line with the earlier observation in *Y11y11* [38].

Chl deficiency resulted in a smaller PSII antenna size in *Y11y11* compared to its wild type Clark by restricting the accumulation of light-harvesting antenna complexes, especially the major light-harvesting antenna LHCII [37]. Concordantly, transgenic *Arabidopsis* plants having low amounts of LHCII displayed low NPQ phenotypes [39,40,41]. Similar antenna downsizing was also found in Chl *b*-less barley *chlorina* mutants [42,43] and *Arabidopsis ch1* [44]. The low NPQ capacity found in MinnGold (Figs. 2d and 5b for Φ_{NPQ}, Tables 1 and 2) is therefore in good agreement with the functional link between NPQ and the Chl-binding antenna complexes.

The NPQ of MinnGold is characterized by a low capacity and slow formation of qE (Table 2). Although slow NPQ relaxation was previously hypothesized for MinnGold [12], the two varieties did not significantly differ in relaxation kinetics of NPQ in our experiments. Different light fluctuation regimes and growth conditions used in [12] and this study may have induced different NPQ levels with different relaxation kinetics.

We found similar, or sometimes even higher, F_v/F_m in MinnGold (Table 1; Table S1), suggesting that the Chl- and NPQ-deficient leaves were apparently not suffering from severer PSII damage under the constant and fluctuating light conditions. A decrease in F_v/F_m is widely used as an indicator of photoinhibition and stress [45]. Interestingly, while decline of F_v/F_m after the 1-h light exposure was no larger in MinnGold than in Eiko (Table S1), lower qPd (Table 1) pointed to increased photoinhibition in MinnGold. The parameter qPd checks the difference between the actual ($F'_{0\ act}$) and calculated (expected) minimal fluorescence yield ($F'_{0\ calc}$; [37]) in the presence of dark-sustained NPQ (Eq. (16); [38]). Unlike F_v/F_m, qPd detects $F'_{0\ act} > F'_{0\ calc}$ resulting from accumulation of permanently closed PSII centers or detachment of unquenched antenna complexes. Lower NPQ and qPd but similar F_v/F_m (Table 1; Table S1) hints at lower dark-sustained antenna quenching in MinnGold. It is worth mentioning that the contribution of PSI to fluorescence level could be different between the two varieties [46]. Thus, new proposed methods taking into account the PSI contribution to F_{yield} should be considered in future works [46,47].

Most likely, other photoprotective mechanisms were compensating for the NPQ deficit in Chl-deficient leaves, as a large pool of carotenoids relative to Chl [43,48,49] and the upregulation of D1 protein repair [50,51]. Higher operational costs of photosynthesis arising from increased photoinhibition and repair [52,53] may have contributed to the growth penalty reported for field-grown plants of MinnGold compared to Eiko [12]. Effects of Chl deficiency on stress resilience need to be investigated in adverse environments, in which both costs and benefits of photoprotection and maintenance increase.

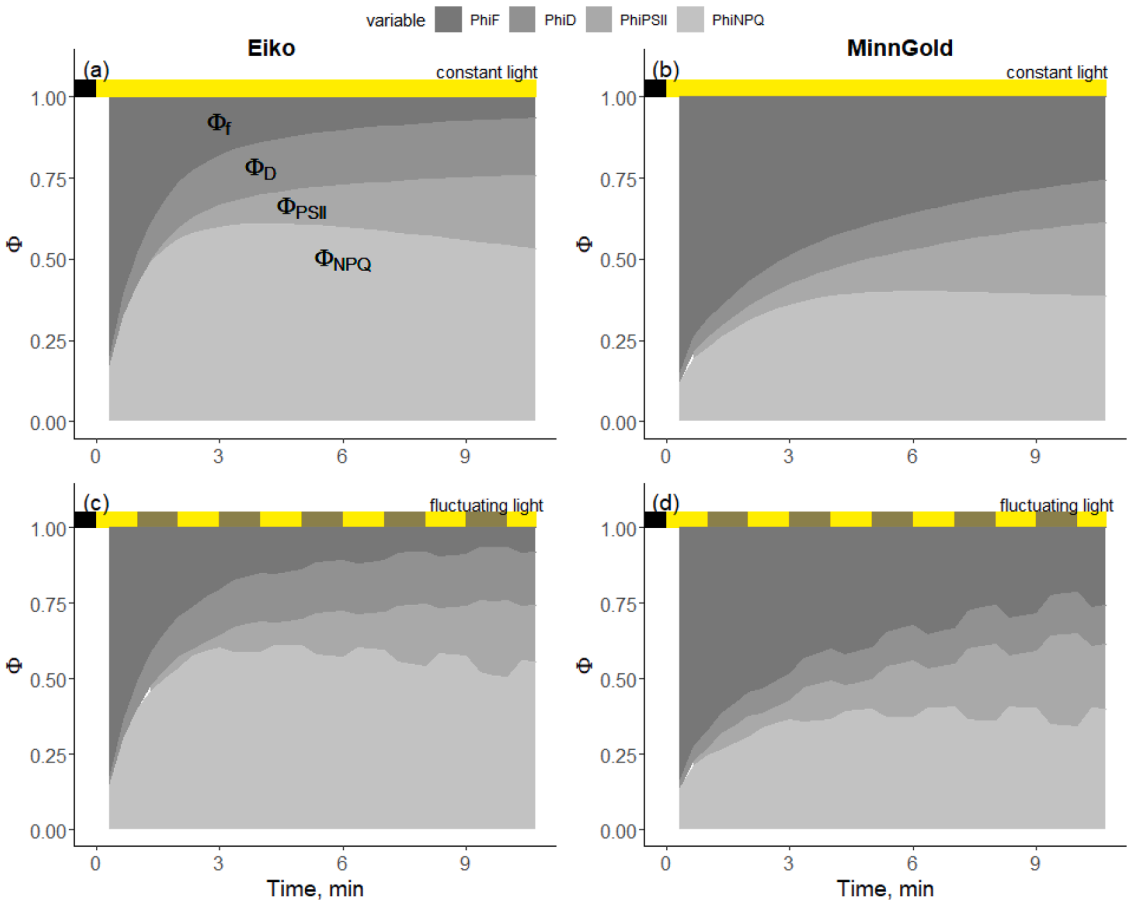

Fig. 4. Energy partitioning of absorbed light in Eiko (a, c) and Chl-deficient mutant MinnGold (b, d) during induction in constant light (a, b) and fluctuating light (c, d). Quantum yield of fluorescence emission (Φ_f), PSII photochemistry (Φ_{PSII}), non-regulated basal heat dissipation (Φ_D) and regulated photoprotective heat dissipation (Φ_{NPQ}) were traced during the initial phase of photosynthetic induction. The partitioning is represented by the areas of different gray scales. The actinic light intensity was set to 650 μmol m^{-2} s^{-1} in the constant light protocol while it was changing between 780 and 520 μmol m^{-2} s^{-1} in the fluctuating light protocol. Data are means of three plants.

Table 2
Kinetic parameters of NPQ in Eiko and MinnGold assessed during dark-to-light transition and after subsequent darkening. The NPQ induction and relaxation were fitted with single or double exponential functions, respectively, according to Eqns. 4 and 5. A single exponential component was found in the induction data, whereas two exponential components were needed to fit the relaxation data. For induction, initial NPQ in the dark (y_0) was set as zero. The values are means ± standard deviations (representing the fitting errors of the respective parameter with n=6). R^2 was >0.8 for induction, >0.9 for relaxation. Different letters show significant differences between the two genotypes at α=0.05.

Type	y_0	A_1	τ_1 (s)	A_2	τ_2 (s)
Induction					
Eiko		2.07 ± 0.09[a]	49.30 ± 6.08 [a]		
MinnGold		1.07 ± 0.03[b]	109.48 ± 14.84 [b]		
Relaxation					
Eiko	0.60 ± 0.37 [a]	0.46 ± 0.06[a]	26.33 ± 9.76 [a]	0.48 ± 0.36 [a]	6086.24 ± 5487.4[a]
MinnGold	0.19 ± 0.14 [a]	0.34 ± 0.03[b]	29.21 ± 6.62 [a]	0.67 ± 0.16 [a]	6204.97 ± 4164.1[a]

How does Chl deficiency affect photosynthetic induction and electron transport?

MinnGold had similar Φ_{PSII} (Fig. 2a) but lower ETR and J_a (Fig. 2e, f) as well as A (Fig. 2g) compared to Eiko because of less light absorption at leaf level [24]. The difference in Φ_{NPQ} between the two plants most clearly manifested itself during the first 10 min of induction (Fig. 5b) when Φ_{PSII} was the same in both (Figs. 2a and 5b), indicating that Φ_{NPQ} was not the reason for the low PSII efficiency during this period. Instead, low g_s (Fig. 2h) was limiting photosynthesis shortly after dark-to-light transition. Notably, the comparison between ETR and J_a yielded a 1:1 correlation (which is expected [54]) during this initial phase (Fig. 3) despite highly variable C_i (Fig. 2i) and the assumptions made in the calculations, such as the factor 0.5 for $fraction_{PSII}$ in Eq. (6) or the value of Γ* borrowed from [34] in Eq. (7).

A good match between ETR and J_a during photosynthetic induction necessitates a feedback regulation to adjust the PSII activity to the needs for NADPH and ATP. Rapid activation of NPQ (Figs. 2d and 5b) serves to dissipate excess light energy as the plastoquinone pool becomes increasingly reduced and PSII reaction centers get closed (Figs. 2b, 2c). Slow and limited induction of NPQ during this period (Table 2) would promote production of reactive oxygen species in MinnGold. After this initial stage, the increase in A (thus also J_a) visibly slowed down in MinnGold (Fig. S3f, g) without a corresponding change in Φ_{PSII} and ETR (Fig. S1a, e), giving rise to the data points above the 1:1 line of Fig. 3. A simple explanation for ETR>J_a is transport of electrons to alternative electron sinks such as the Mehler reaction [31]. The transient deceleration of A rise (Fig. 2g) may have promoted electron transport to other sinks. Overestimation of $fraction_{PSII}$ * α (set as 0.5 * 0.55 for MinnGold) is another possible scenario for ETR>J_a. The energy partitioning between PSII and PSI ($fraction_{PSII}$), on the other hand, is modulated by relative abundance of these photosystem complexes and state transitions [55].

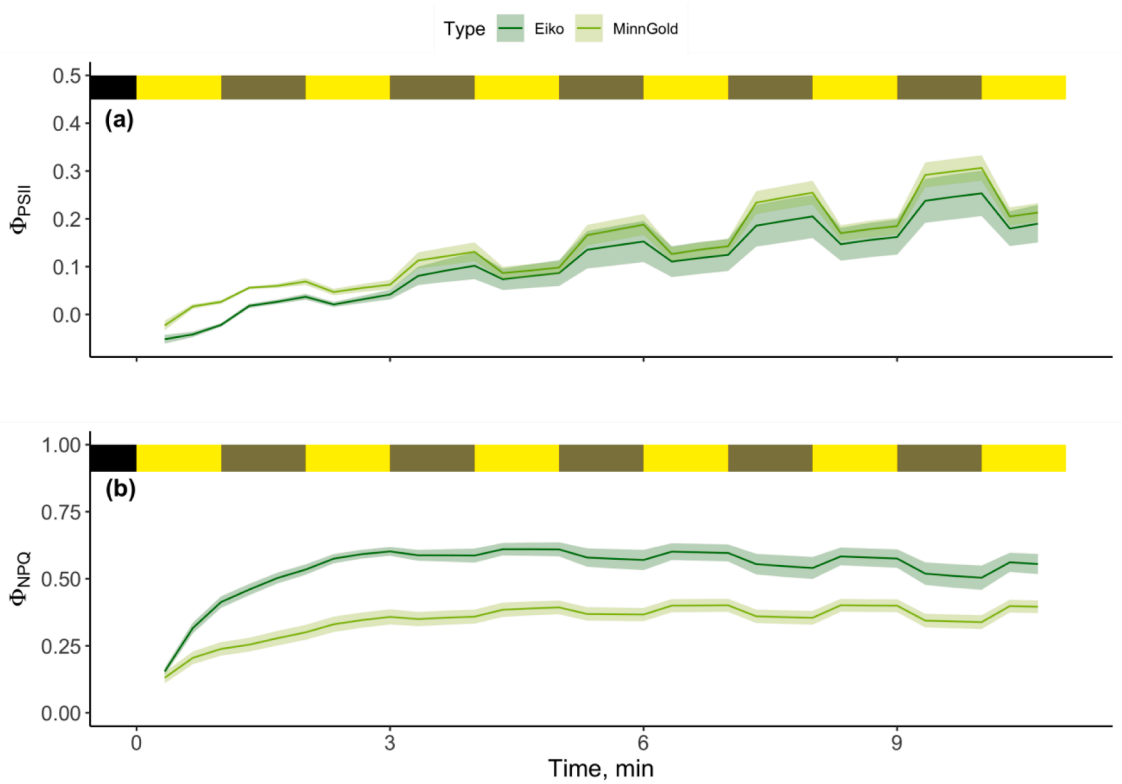

Fig. 5. Operating efficiency of photosystem II (Φ_{PSII}; a) and non-photochemical quenching (Φ_{NPQ}; b) traced during the initial phase of photosynthetic induction under fluctuating light in Eiko and Chl-deficient mutant MinnGold. The light intensity was fluctuating between 780 μmol m^{-2} s^{-1} (yellow) and 520 μmol m^{-2} s^{-1} (gray) with a period of 1 min. The solid lines represents the average, the pale areas show the standard errors (n=3).

We suggest that these measurements should be measured in future experiments relating Chl-deficient plant to photosynthesis. Yet, Chl-deficient MinnGold, like the Chl *b*-less (LHCII-less) barley *chlorina* mutant [56], is unlikely to do more state transitions than Eiko does. Since ChlF analysis mostly reflects signals from chloroplasts in upper cell layers that are close to the measurement surface, discrepancy between ETR and J_a (ETR>J_a) may arise, especially when using blue light that is strongly absorbed by upper-layer chloroplasts [57]. Nevertheless, the light used in this experiment is only 6% blue light. We also did observe a ~2.5 % higher intensity of saturating flash recorded in MinnGold (Fig. S6), likely resulting from the higher reflectance of Chl-deficient leaves which may have affected the determination of Φ_{PSII} and thus ETR. While we cannot rule out the possible effects of chloroplast movement and carotenoid absorption, assuming that the transient slowdown of *A* increase (Fig. 2f) is the direct cause of ETR>J_a in the Chl-deficient leaves, alternative electron sinks seem to be the most probable explanatio

As the induction curves approached the steady state, the correlation between ETR and Ja started to deviate from the 1:1 line in both varieties (Fig. 3). At this stage, ChlF was underestimating ETR regardless of the leaf Chl contents. None of the aforementioned sources of discrepancy can account for ETR<Ja. Yet the substantially higher steady-state value of fractionPSII * α seen in Fig. S4 than used in Eq. (6) may be due to imbalance in light energy distribution between PSII and PSI, this is difficult to reconcile with liner electron transport. Looking at the kinetics of Fm' (data not shown), we observed unsteady kinetics at the initial stage of induction, indicating a non-saturating pulses. We therefore suspect that ETR<Ja was due to underestimated levels of Fm'. Furthermore, the protocol applied for the fluorescence measurements (180 saturating pulses during the light treatment and 18 during the dark treatment) may have potentially affected the trace and therefore, in future works, it would be vital to check how the interval between pulses affect the fluorescence kinetic.

For these reasons, we focused our analysis on the first 11 minutes of the experiment, in which ETR is not substantially lower than J_a (Fig. 3). The data further this point are only shown in supplementary Figs., since the trend still shows good agreement with the gas-exchange data.

It has been suggested that reduced light absorption of Chl-deficient leaves may improve canopy-level photosynthesis by allowing deeper light penetration into the canopy [58]. However, *Y11y11* and its wild type Clark showed similar canopy photosynthesis in the field [6] and so did MinnGold and Eiko [12, [59] in non-fluctuating light]. For MinnGold, no increase in canopy photosynthesis may be explained by lower ETR and *A* at leaf level (Fig. 2e, f, g). For *Y11y11*, in contrast, leaf-level photosynthesis (as well as NPQ) was comparable with Clark [6]. A simulation study based on 67 soybean accessions with varying leaf Chl contents has predicted no drawback, but also no gain, in canopy photosynthesis by Chl deficiency [60] due to non-optimal N distribution inside the canopy. The contrasting photosynthesis and NPQ phenotypes found in MinnGold (this study and [12]) and *Y11y11* [6] at leaf level are probably related to different genetic backgrounds, in addition to the allelic effects of ChlI1a [61]. Comparative studies using MinnGold and *Y11y11* as well as Clark and the parental lines of MinnGold (M99-274166 and MN0091; [861]) may reveal factors that determine photosynthetic and photoprotective capacities of Chl-deficient leaves.

How does Chl deficiency affect the apparent yield of fluorescence emission?

Chl-deficient leaves of MinnGold had higher Φ_f at PSII and lower apparent F_{yield} at leaf level (Table 1). The decrease in the apparent F_{yield} is probably a consequence of the dramatically reduced Chl content and thus light absorption. This dominant effect of low Chl content on lower F_{yield}, which contradicted the increase in Φ_f in MinnGold, exemplifies the focal point at which estimating aPAR is necessary to derive F_{yield}. Following the emission by Chl molecules, various factors can influence

F_{yield} when it is detected from outside the leaf surface or the canopy which are critical when analyzing passive ChlF signal such as SIF. Several studies retrieving SIF at canopy and regional scale showed high degree of correlation between SIF and gross primary production, which has been explained by the correlation between Chl content (per leaf area) and photosynthetic light absorption [62,63]. However, such a correlation is not always valid at higher Chl contents where the relationship between SIF and Chl saturates [64]. Our results highlight the importance of parameterizing SIF signals based on the Chl level and absorbed light, while properly accounting for reabsorption [65] and the exit probability of ChlF photons [66]. For standardization, we suggest to apply the formula of [67] and use the efficiency of energy transfer within the system to link Φ_f to the apparent F_{yield}.

Conclusions

Comparing leaf-level ChlF and gas exchange parameters between MinnGold and green Eiko indicated slower induction and reduced capacity of NPQ as well as slower photosynthetic induction in Chl-deficient leaves of MinnGold, which may explain the lower biomass of this variety in the field. Contrary to the previous studies [12,13], we did not observe slower NPQ relaxation in MinnGold, which may be due to different growth and experimental conditions used. In the context of remote sensing plant productivity, our results from comparing photosynthesis of Eiko and MinnGold provide a mechanistic understanding on how to link passive SIF to productivity fluxes. Models like Soil-Canopy-Observation of Photochemistry and Energy fluxes (SCOPE, [68]) will help combine and elucidate relationship between SIF, Chl content and productivity on plant scale or on ecosystem scale using a big leaf model.

Funding

G.A. and N.S. was supported by funds of the University of Udine for their mission to Forschungszentrum Jülich GmbH; System development was funded by PDM_VQR3_DI4A_MISSIONI; G.A., N.S. and A.P. have been also supported by the Italian Government through the NextGenerationEU funds (DM 737/2021). Open access is funded by the Deutsche Forschungsgemeinschaft (DFG, German Research Foundation) – 491111487]

Declaration of Competing Interest

The authors declare that they have no known competing financial interests or personal relationships that could have appeared to influence the work reported in this paper.

Data Availability

Data will be made available on request.

Acknowledgements

We would like to thank Ladislav Nedbal, MaPi Cendrero-Pilar, Karolina Sakowska and Franco Miglietta for insightful discussions.

Supplementary materials

Supplementary material associated with this article can be found, in the online version, at doi:10.1016/j.jpap.2022.100152.

References

[1] L. Genesio, R. Bassi, F. Miglietta, Plants with less chlorophyll: A global change perspective, Glob. Chang. Biol. gcb. 15470 (2020), https://doi.org/10.1111/gcb.15470.
[2] E. Lugato, A. Cescatti, A. Jones, G. Ceccherini, G. Duveiller, Maximising climate mitigation potential by carbon and radiative agricultural land management with cover crops, Environ. Res. Lett. 15 (2020), 094075, https://doi.org/10.1088/1748-9326/aba137.
[3] H. Croft, J.M. Chen, X. Luo, P. Bartlett, B. Chen, R.M. Staebler, Leaf chlorophyll content as a proxy for leaf photosynthetic capacity, Glob. Chang. Biol. 23 (2017) 3513–3524, https://doi.org/10.1111/gcb.13599.
[4] J. Gu, Z. Zhou, Z. Li, Y. Chen, Z. Wang, H. Zhang, Rice (*Oryza sativa* L.) with reduced chlorophyll content exhibit higher photosynthetic rate and efficiency, improved canopy light distribution, and greater yields than normally pigmented plants, F. Crop. Res. 200 (2017) 58–70, https://doi.org/10.1016/j.fcr.2016.10.008.
[5] J.S. Paixão, J.R. Da Silva, K.F. Ruas, W.P. Rodrigues, J.A.M. Filho, W.de P. Bernado, D.P. Abreu, L.S. Ferreira, J.C. Gonzalez, K.L. Griffin, J.C. Ramalho, E. Campostrini, Photosynthetic capacity, leaf respiration and growth in two papaya (*Carica papaya*) genotypes with different leaf chlorophyll concentrations, AoB Plants 11 (2019), https://doi.org/10.1093/aobpla/plz013.
[6] R.A. Slattery, A. VanLoocke, C.J. Bernacchi, X.-G. Zhu, D.R. Ort, Photosynthesis, light use efficiency, and yield of reduced-chlorophyll soybean mutants in field conditions, Front. Plant Sci. 8 (2017) 549, https://doi.org/10.3389/fpls.2017.00549.
[7] S.P. Long, X.-G. Zhu, S.L. Naidu, D.R. Ort, Can improvement in photosynthesis increase crop yields? Plant, Cell Environ. 29 (2006) 315–330, https://doi.org/10.1111/j.1365-3040.2005.01493.x.
[8] D.R. Ort, X. Zhu, A. Melis, X. Zhu, A. Melis, Optimizing antenna size to maximize photosynthetic efficiency, Plant Physiol. 155 (2011) 79–85, https://doi.org/10.1104/pp.110.165886.
[9] D.R. Ort, S.S. Merchant, J. Alric, A. Barkan, R.E. Blankenship, R. Bock, R. Croce, M. R. Hanson, J.M. Hibberd, S.P. Long, T.A. Moore, J. Moroney, K.K. Niyogi, M.A. J. Parry, P.P. Peralta-Yahya, R.C. Prince, K.E. Redding, M.H. Spalding, K.J. van Wijk, W.F.J. Vermaas, S. Von Caemmerer, A.P.M. Weber, T.O. Yeates, J.S. Yuan, X. G. Zhu, Redesigning photosynthesis to sustainably meet global food and bioenergy demand, Proc. Natl. Acad. Sci. 112 (2015) 8529–8536, https://doi.org/10.1073/pnas.1424031112.
[10] S.P. Long, A. Marshall-Colon, X.G. Zhu, Meeting the global food demand of the future by engineering crop photosynthesis and yield potential, Cell (2015), https://doi.org/10.1016/j.cell.2015.03.019.
[11] S. Zhang, X. Wu, J. Cui, F. Zhang, X. Wan, Q. Liu, Y. Zhong, T. Lin, Physiological and transcriptomic analysis of yellow leaf coloration in Populus deltoides Marsh, PLoS One 14 (2019), e0216879, https://doi.org/10.1371/journal.pone.0216879.
[12] K. Sakowska, G. Alberti, L. Genesio, A. Peressotti, G. Delle Vedove, D. Gianelle, R. Colombo, M. Rodeghiero, C. Panigada, R. Juszczak, M. Celesti, M. Rossini, M. Haworth, B.W. Campbell, J.-P. Mevy, L. Vescovo, M.P. Cendrero-Mateo, U. Rascher, F. Miglietta, Leaf and canopy photosynthesis of a chlorophyll deficient soybean mutant, Plant Cell Environ. 41 (2018), https://doi.org/10.1111/pce.13180.
[13] L. Genesio, R.M. Bright, G. Alberti, A. Peressotti, G. Delle Vedove, G. Incerti, P. Toscano, M. Rinaldi, O. Muller, F. Miglietta, A chlorophyll-deficient, highly reflective soybean mutant: radiative forcing and yield gaps, Environ. Res. Lett. 15 (2020), 074014, https://doi.org/10.1088/1748-9326/ab865e.
[14] Y. Wang, S.J. Burgess, E.M. de Becker, S.P. Long, Photosynthesis in the fleeting shadows: an overlooked opportunity for increasing crop productivity? Plant J. 101 (4) (2020) 874–884, https://doi.org/10.1111/tpj.14663.
[15] A.P. De Souza, S.J. Burgess, L. Doran, J. Hansen, L. Manukyan, N. Maryn, D. Gotarkar, L. Leonelli, K.K. Niyogi, S.P. Long, Soybean photosynthesis and crop yield are improved by accelerating recovery from photoprotection, Science 377 (6608) (2022) 851–854, https://doi.org/10.1126/science.adc9831.
[16] W. Yamori, Photosynthetic response to fluctuating environments and photoprotective strategies under abiotic stress, J. Plant Res. 129 (3) (2016) 379–395, https://doi.org/10.1007/s10265-016-0816-1.
[17] J. Kromdijk, K. Głowacka, L. Leonelli, S.T. Gabilly, M. Iwai, K.K. Niyogi, S.P. Long, Improving photosynthesis and crop productivity by accelerating recovery from photoprotection, Science 354 (6314) (2016) 857–861, https://doi.org/10.1126/science.aai8878.
[18] A. Garcia-Molina, D. Leister, Accelerated relaxation of photoprotection impairs biomass accumulation in Arabidopsis, Nat. Plants 6 (2020) 9–12, https://doi.org/10.1038/s41477-019-0572-z.
[19] A. Porcar-Castell, E. Tyystjärvi, J. Atherton, C. Van der Tol, J. Flexas, E.E. Pfündel, J. Moreno, C. Frankenberg, J.A. Berry, Linking chlorophyll a fluorescence to photosynthesis for remote sensing applications: mechanisms and challenges, J. Experimen. Botany 65 (15) (2014) 4065–4095, https://doi.org/10.1093/jxb/eru191.
[20] A. Stirbet, Excitonic connectivity between photosystem II units: What is it, and how to measure it? Photosynth. Res. 116 (2013) 189–214, https://doi.org/10.1007/s11120-013-9863-9.
[21] D.M. Kramer, G. Johnson, O. Kiirats, G.E. Edwards, New fluorescence parameters for the determination of QA redox state and excitation energy fluxes, Biol. Chem. (2004) 209–218, https://doi.org/10.1023/B:PRES.0000015391.99477.0d.
[22] N.R. Baker, Chlorophyll fluorescence: a probe of photosynthesis in vivo, Annu. Rev. Plant Biol. 59 (2008) 89–113.

[23] I. Kasajima, K. Takahara, M. Kawai-Yamada, H. Uchimiya, Estimation of the relative sizes of rate constants for chlorophyll de-excitation processes through comparison of inverse fluorescence intensities, Plant Cell Physiol. 50 (2009) 1600–1616.
[24] Salvatori, N., Giorgio, A., Muller, O., Rascher, U., Peressotti, A., 2021. A low-cost automated growth chamber system for continuous measurements of gas exchange at canopy scale in dynamic conditions. Plant Methods 17, 69. https://doi.org/10.1186/s13007-021-00772-z.
[25] S.R. Vialet-Chabrand, J.S. Matthews, L. McAusland, M.R. Blatt, H. Griffiths, T. Lawson, Temporal dynamics of stomatal behavior: modeling and implications for photosynthesis and water use, Plant Physiol. 174 (2) (2017) 603–613, https://doi.org/10.1104/pp.17.00125.
[26] M.B.W.L. Kitajima, W.L. Butler, Quenching of chlorophyll fluorescence and primary photochemistry in chloroplasts by dibromothymoquinone, Biochimica et Biophysica Acta (BBA)-Bioenergetics 376 (1) (1975) 105–115.
[27] B. Genty, J.M. Briantais, N.R. Baker, The relationship between the quantum yield of photosynthetic electron transport and quenching of chlorophyll fluorescence, Biochim. Biophys. Acta - Gen. Subj. 990 (1989) 87–92, https://doi.org/10.1016/S0304-4165(89)80016-9.
[28] W. Bilger, O. Björkman, Role of the xanthophyll cycle in photoprotection elucidated by measurements of light-induced absorbance changes, fluorescence and photosynthesis in leaves of Hedera canariensis, Photosynth. Res. 25 (1990) 173–185, https://doi.org/10.1007/BF00033159.
[29] M. Nilkens, E. Kress, P. Lambrev, Y. Miloslavina, M. Müller, A.R. Holzwarth, P. Jahns, Identification of a slowly inducible zeaxanthin-dependent component of non-photochemical quenching of chlorophyll fluorescence generated under steady-state conditions in Arabidopsis, Biochimica et Biophysica Acta (BBA)-Bioenergetics 1797 (4) (2010) 466–475, https://doi.org/10.1016/j.bbabio.2010.01.001.
[30] J.P. Krall, G.E. Edwards, Relationship between photosystem II activity and CO2 fixation in leaves, Physiologia Plantarum 86 (1) (1992) 180–187, https://doi.org/10.1111/j.1399-3054.1992.tb01328.x.
[31] S. von Caemmerer, G.D. Farquhar, Some relationships between the biochemistry of photosynthesis and the gas exchange of leaves, Planta (1981) 376–387, https://doi.org/10.1007/BF00384257.
[32] N.R. Baker, Chlorophyll fluorescence: a probe of photosynthesis in vivo, Annu. Rev. Plant Biol. 59 (2008) 89–113, https://doi.org/10.1146/annurev.arplant.59.032607.092759.
[33] G.D. Farquhar, S. von Caemmerer, J.A. Berry, A biochemical model of photosynthetic CO2 assimilation in leaves of C3 species, Planta 149 (1980) 78–90, https://doi.org/10.1007/BF00386231.
[34] B.J. Walker, D.R. Ort, Improved method for measuring the apparent CO_2 photocompensation point resolves the impact of multiple internal conductances to CO_2 to net gas exchange, Plant Cell Environ. 38 (2015) 2462–2474, https://doi.org/10.1111/pce.12562.
[35] B.A. Kimball, in: Impact of carbon dioxide, trace gases, and climate change on global agriculture: proceedings of a symposium, American Society of Agronomy, 1990.
[36] L. Hendrickson, R.T. Furbank, W.S. Chow, A simple alternative approach to assessing the fate of absorbed light energy using chlorophyll fluorescence, Photosynth. Res. 82 (1) (2004) 73–81, https://doi.org/10.1023/B:PRES.0000040446.87305.f4.
[37] K. Oxborough, N.R. Baker, Resolving chlorophyll *a* fluorescence images of photosynthetic efficiency into photochemical and non-photochemical components – calculation of qP and Fv-/Fm-; without measuring F_O, Photosynth. Res. 54 (1997) 135–142, https://doi.org/10.1023/A:1005936823310.
[38] A.V. Ruban, E.H. Murchie, Assessing the photoprotective effectiveness of non-photochemical chlorophyll fluorescence quenching: A new approach, Biochim. Biophys. Acta - Bioenerg. 1817 (2012) 977–982, https://doi.org/10.1016/j.bbabio.2012.03.026.
[39] J. Andersson, M. Wentworth, R.G. Walters, C.A. Howard, A.V. Ruban, P. Horton, S. Jansson, Absence of the Lhcb1 and Lhcb2 proteins of the light-harvesting complex of photosystem II – effects on photosynthesis, grana stacking and fitness, Plant J. 35 (2003) 350–361.
[40] M. Pietrzykowska, M. Suorsa, D.A. Semchonok, M. Tikkanen, E.J. Boekema, E.-M. Aro, S. Jansson, The light-harvesting chlorophyll *a/b* binding proteins Lhcb1 and Lhcb2 play complementary roles during state transitions in Arabidopsis, Plant Cell 26 (2014) 3646–3660.
[41] L. Nicol, W.J. Nawrocki, R. Croce, Disentangling the sites of non-photochemical quenching in vascular plants, Nat. Plants 5 (11) (2019) 1177–1183, https://doi.org/10.1038/s41477-019-0526-5.
[42] S. Falk, D. Bruce, N.P.A. Huner, Photosynthetic performance and fluorescence in relation to antenna size and absorption cross-sections in rye and barley grown under normal and intermittent light conditions, Photosynth. Res. 42 (1994) 145–155, https://doi.org/10.1007/BF02187125.
[43] M. Król, M.D. Spangfort, N.P.A. Huner, G. Öquist, P. Gustafsson, S. Jansson, Chlorophyll *a/b*-binding proteins, pigment conversions, and early light-induced proteins in a chlrophyll *b*-less barley mutant, Plant Pysiol 107 (1995) 873–883, https://doi.org/10.1104/pp.107.3.873.
[44] M. Havaux, L. Dall'Osto, R. Bassi, Zeaxanthin has enhanced antioxidant capacity with respect to all other xanthophylls in Arabidopsis leaves and functions independent of binding to PSII antennae, Plant Cell 145 (2007) 1506–1520, https://doi.org/10.1104/pp.107.108480.
[45] N.R. Baker, E. Rosenqvist, Applications of chlorophyll fluorescence can improve crop production strategies: an examination of future possibilities, J. Exp. Bot. 55 (2004) 1607–1621, https://doi.org/10.1093/jxb/erh196.
[46] E.E. Pfündel, Simultaneously measuring pulse-amplitude-modulated (PAM) chlorophyll fluorescence of leaves at wavelengths shorter and longer than 700 nm, Photosynth. Res. 147 (3) (2021) 345–358, https://doi.org/10.1007/s11120-021-00821-7.
[47] V. Giovagnetti, M.A. Ware, A.V. Ruban, Assessment of the impact of photosystem I chlorophyll fluorescence on the pulse-amplitude modulated quenching analysis in leaves of Arabidopsis thaliana, Photosynth. Res. 125 (1) (2015) 179–189, https://doi.org/10.1007/s11120-015-0087-z.
[48] H. Härtel, H. Lokstein, B. Grimm, B. Rank, Kinetic studies on the xanthophyll cycle in barley leaves, Plant Physiol. 110 (1996) 471–482, https://doi.org/10.1104/pp.110.2.471.
[49] R. Esteban, O. Barrutia, U. Artetxe, B. Fernández-Marín, A. Hernández, J.I. García-Plazaola, Internal and external factors affecting photosynthetic pigment composition in plants: a meta-analytical approach, New Phytol. 206 (2015) 268–280, https://doi.org/10.1111/nph.13186.
[50] A. Melis, Photosystem –II damage and repair cycle in chloroplasts: what modulates the rate of photodamage in vivo? Trends Plant Sci. 4 (1999) 130–135, https://doi.org/10.1016/s1360-1385(99)01387-4.
[51] M.A. Gururani, J. Venkatesh, L.-S.P. Tran, Regulation of photosynthesis during abiotic stress-induced photoinhibition, Mol. Plant 8 (2015) 1304–1320, https://doi.org/10.1016/j.molp.2015.05.005.
[52] J. Raven, The cost of photoinhibition, Physiol. Plant. 142 (2011) 87–104, https://doi.org/10.1111/j.1399-3054.2011.01465.x.
[53] K. Miyata, K. Noguchi, I. Terashima, Cost and benefit of the repair of photodamaged photosystem II in spinach leaves: roles of acclimation to growth light, Photosynth. Res. 113 (2012) 165–180, https://doi.org/10.1007/s11120-012-9767-0.
[54] C.J. Bernacchi, C. Pimentel, S.P. Long, In vivo temperature response functions of parameters required to model RuBP-limited photosynthesis, Plant Cell Environ 26 (2003) 1419–1430, https://doi.org/10.1046/j.0016-8025.2003.01050.x.
[55] S. Bellafiore, F. Barneche, G. Peltier, J.-D. Rochaix, State transitions and light adaptation require chloroplast thylakoid protein kinase STN7, Nature 433 (2005) 892–895, https://doi.org/10.1038/nature03286.
[56] B. Osmond, W.S. Chow, B.J. Pogson, S.A. Robinson, Probing functional and optical cross-sections of PSII in leaves during state transitions using fast repetition rate light induced fluorescence transients, Funct. Plant Biol. 46 (6) (2019) 567–583, https://doi.org/10.1071/FP18054.
[57] J.R. Evans, Potential errors in electron transport rates calculated from chlorophyll fluorescence as revealed by a multilayer leaf model, Plant Cell Physiol. 50 (2009) 698–706, https://doi.org/10.1093/pcp/pcp041.
[58] D.T. Drewry, P. Kumar, S.P. Long, Simultaneous improvement in productivity, water use, and albedo through crop structural modification, Global Change Biol. 20 (2014) 1955–1967, https://doi.org/10.1111/gcb.12567.
[59] N. Salvatori, G. Alberti, O. Muller, A. Peressotti, Does fluctuating light affect crop yield? A Focus Dyn. Photosynth. Two Soybean Varieties (2022) https://doi.org/10.3389/fpls.2022.862275.
[60] B.J. Walker, D.T. Drewry, R.A. Slattery, A. VanLoocke, Y.B. Cho, D.R. Ort, Chlorophyll can be reduced in crop canopies with little penalty to photosynthesis, Plant Physiol. 176 (2018) 1215–1232, https://doi.org/10.1104/pp.17.01401.
[61] B.W. Campbell, D. Mani, S.J. Curtin, R.A. Slattery, J.-M. Michno, D.R. Ort, P. J. Schaus, R.G. Palmer, J.H. Orf, R.M. Stupar, Identical substitutions in magnesium chelatase paralogs result in chlorophyll-deficient soybean mutants, G3 (Bethesda) 5 (2014) 123–131, https://doi.org/10.1534/g3.114.015255.
[62] Goulas, Y., Fournier, A., Daumard, F., Champagne, S., Ounis, A., Marloie, O., Moya, I., 2017. Gross primary production of a wheat canopy relates stronger to far red than to red solar-induced chlorophyll fluorescence 1–31. https://doi.org/10.3390/rs9010097.
[63] K. Yang, Y. Ryu, B. Dechant, J.A. Berry, Y. Hwang, C. Jiang, M. Kang, J. Kim, H. Kimm, A. Kornfeld, X. Yang, Remote Sensing of Environment Sun-induced chlorophyll fluorescence is more strongly related to absorbed light than to photosynthesis at half-hourly resolution in a rice paddy, Remote Sens. Environ. 216 (2018) 658–673, https://doi.org/10.1016/j.rse.2018.07.008.
[64] U. Rascher, L. Alonso, A. Burkart, C. Cilia, S. Cogliati, R. Colombo, A. Damm, M. Drusch, L. Guanter, J. Hanus, T. Hyvärinen, T. Julitta, J. Jussila, K. Kataja, P. Kokkalis, S. Kraft, T. Kraska, M. Matveeva, J. Moreno, O. Muller, C. Panigada, M. Pikl, F. Pinto, L. Prey, R. Pude, M. Rossini, A. Schickling, U. Schurr, D. Schüttemeyer, J. Verrelst, F. Zemek, Sun-induced fluorescence–a new probe of photosynthesis: First maps from the imaging spectrometer HyPlant, Global Change Biol. 21 (12) (2015) 4673–4684, https://doi.org/10.1111/gcb.13017.
[65] A.A. Gitelson, C. Buschmann, H.K. Lichtenthaler, Leaf chlorophyll fluorescence corrected for re-absorption by means of absorption and reflectance measurements, J. Plant Physiol. 152 (2-3) (1998) 283–296, https://doi.org/10.1016/S0176-1617(98)80143-0.
[66] Y. Zeng, G. Badgley, B. Dechant, Y. Ryu, M. Chen, Remote sensing of environment a practical approach for estimating the escape ratio of near-infrared solar- induced chlorophyll fluorescence, Remote Sens. Environ. (2019), 111209, https://doi.org/10.1016/j.rse.2019.05.028.
[67] K.-L. Wong, G.B. Jean-Claude, P.A. Tanner, Quantum yield and brightness, J. Luminescence 224 (2020), 117256, https://doi.org/10.1016/j.jlumin.2020.117256.
[68] C. Van der Tol, J.A. Berry, P.K.E. Campbell, U. Rascher, Models of fluorescence and photosynthesis for interpreting measurements of solar-induced chlorophyll fluorescence, J. Geophys. Res. Biogeosci. 119 (12) (2014) 2312–2327, https://doi.org/10.1002/2014JG002713.